Progress In Electromagnetics Research B, Vol. 42, 1–22, 2012

THEORETICAL EXAMINATION OF ELECTROMAGNETIC WAVE TUNNELING THROUGH CASCADED ϵ- AND μ-NEGATIVE METAMATERIAL SLABS

C. H. Liu* **and N. Behdad**

Department of Electrical and Computer Engineering, University of Wisconsin-Madison, 1415 Engineering Drive, Madison, WI 53706, USA

Abstract—In this paper, we examine the close relationship that exists between the phenomenon of electromagnetic (EM) wave tunneling through stacks of single-negative metamaterial slabs and classical microwave filter theory. In particular, we examine the propagation of EM waves through a generalized multi-layer structure composed of N ϵ-negative layers separated from each other by $N-1$ μ-negative layers, where $N \geq 2$ is a positive integer. We demonstrate that, if certain conditions are met, this multi-layer structure can act as a capacitively-coupled, coupled-resonator filter with an Nth-order bandpass response. Exploiting this relationship, we develop a generalized, analytical synthesis method that can be used to determine the physical parameters of this structure from its *a priori* known frequency response. We present several design examples in conjunction with numerical EM simulation results to demonstrate the validity of this analogy and examine the accuracy of the proposed synthesis procedure.

1. INTRODUCTION

Electromagnetic (EM) waves cannot propagate over several skin depths† in materials exhibiting negative permittivity or negative permeability values (also known as single-negative (SNG) materials). EM waves that enter SNG materials exponentially decay along the direction of propagation and rapidly loose their energy. However, when SNG slabs are used in a suitably-designed multi-layer structure, they can be made completely transparent and allow for the total

Received 10 May 2012, Accepted 20 June 2012, Scheduled 25 June 2012

* Corresponding author: Chien-Hao Liu (cliu82@wisc.edu).

† Skin depth is the distance that an EM wave travels in a lossy material and its value reduces to e^{-1} or 36.8%.

transmission of electromagnetic waves. Complete transmission of EM waves through these propagation barriers is often referred to as EM wave tunneling due to its analogous nature to quantum tunneling problems. EM wave tunneling through such propagation barriers has been extensively investigated over the years[‡]. Early investigations of this phenomenon focused on the propagation of EM waves through naturally occurring SNG materials such as plasmas [1] or metallic films [2]. With the emergence of the field of metamaterials in recent years, however, major advancements have been made in synthesizing materials with any desired permittivity or permeability values. Therefore, the idea of EM wave tunneling through metamaterial layers having negative permittivity (ϵ-negative or ENG) or negative permeability (μ-negative or MNG) values has received significant attention in the past decade [3–19]. Studies conducted in this area have examined various multi-layer structures composed of ENG, MNG, and/or double-positive (DPS) materials. Examples include tunneling through ENG layers paired with MNG ones [3, 11, 12], tunneling through an ENG layer separated from an MNG layer with free space [14], and tunneling through multi-layer structures composed of SNG and double-positive (DPS) layers [9, 10, 18].

Despite the large number of studies conducted in this area to date, few of them provide any in-depth examination of the close relationship that exists between such tunneling problems and classical microwave filters. Such an examination is important for two reasons. First, it provides a simple and easy-to-understand method for explaining a rather complicated physical phenomenon. Additionally, by exploiting this analogy, a synthesis procedure can be developed[§] and used for determining the physical parameters of the multi-layer structure that will result in an *a priori* known desired frequency response. In this paper, we examine the problem of electromagnetic wave tunneling through a generalized multi-layer structure composed of multiple cascaded ENG and MNG layers. The structure considered here is composed of N, ENG layers that are separated from one another with $N-1$ MNG layers. N is an arbitrary positive integer and $N \geq 2$. We propose an equivalent circuit model for this multi-layer composite structure and demonstrate that if certain conditions are met, this structure becomes equivalent to capacitively-coupled, coupled-resonator bandpass filter of order N. By establishing this relationship, we develop an analytical procedure for determining the physical parameters of structure that will result in a given *a priori* known transfer function. We verify the validity of the proposed

[‡] In earlier investigations, the keyword tunneling is used less frequently.
[§] The synthesis procedure will be unique to the specific tunneling problem considered.

synthesis procedure using full-wave numerical EM simulations and examine the conditions that must be met to ensure that this analogy remains valid. Finally, we extend the proposed synthesis procedure to multi-layer structures composed of N MNG slabs sandwiching $N-1$ ENG slabs through the use of the duality principle.

2. PROBLEM DEFINITION

Figure 1(a) shows the three dimensional (3D) topology of the problem considered in this paper. The structure consists of planar MNG layers separated from each other by very thin ENG layers. Each layer extends to infinity along the x and y directions but has finite thickness along z direction. In our theoretical analysis in this paper, we assume that each layer is isotropic, linear, and homogeneous. The relative permittivity of each ENG layer is described by a lossless Drude model ($\epsilon_{\mathrm{ENG}} = 1 - \omega_{\mathrm{ENG}}^2/\omega^2$) where $\omega_{\mathrm{ENG}}/(2\pi)$ is the electric plasma frequency. The relative permeability of the ENG layer, μ_{ENG}, is assumed to be constant. Similarly, the relative permeability of each MNG layer is described by a lossless Drude model, $\mu_{\mathrm{MNG}} = 1 - \omega_{\mathrm{MNG}}^2/\omega^2$ where $\omega_{\mathrm{MNG}}/(2\pi)$ is the magnetic plasma frequency. The relative permittivity of the MNG layers, ϵ_{MNG}, is assumed to be

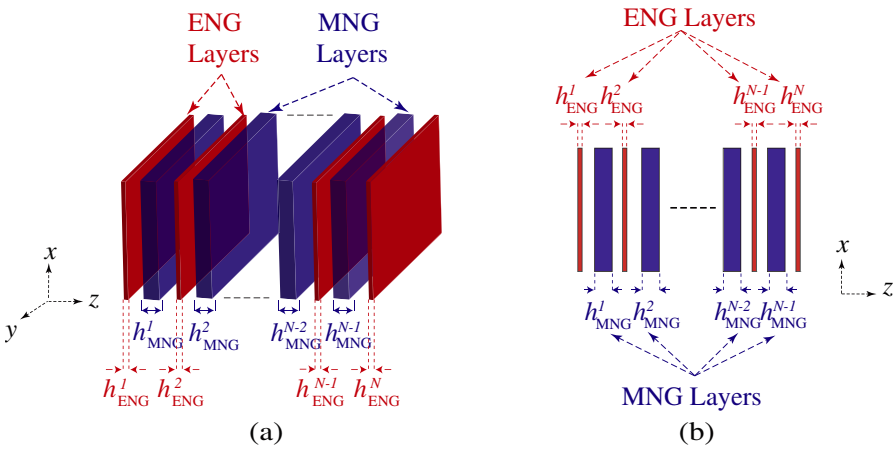

Figure 1. (a) 3D topology of the generalized electromagnetic wave tunneling problem considered in this paper. This multi-layer structure consists of $N-1$ MNG layers sandwiched by N ENG layers. Each layer extends to infinity along x and y directions but has finite thickness along the z direction. (b) Side view of the multi-layer structure.

constant. The ENG (MNG) layers become opaque at frequency bands that fall below their electric (magnetic) plasma frequencies where the relative permittivity (relative permeability) values are negative. Additionally, the different ENG (MNG) layers are not necessarily identical to each other and can have different thicknesses and plasma frequencies.

To examine the propagation of electromagnetic waves through this multi-layer structure, we adopt a simple circuit-based analysis method. Figure 2(a) shows a transmission-line-based equivalent circuit model for this structure which is valid for a vertically incident transverse electromagnetic (TEM) wave. Here, the MNG layers are modeled with transmission lines with lengths of $h^1_{\rm MNG}$, $h^2_{\rm MNG}$, ..., $h^{N-1}_{\rm MNG}$ and characteristic impedances of $Z^1_{\rm MNG}$, $Z^2_{\rm MNG}$, ..., $Z^{N-1}_{\rm MNG}$. The ENG layers are modeled with transmission lines with lengths of $h^1_{\rm ENG}$, ..., $h^N_{\rm ENG}$ and characteristic impedances of $Z^1_{\rm ENG}$, ..., $Z^N_{\rm ENG}$. The semi-infinite spaces on the both sides of the composite ENG-MNG multi-layer structure are modeled with semi-infinite transmission lines with characteristic impedances of Z_0, where $Z_0 = 377\,\Omega$. The transmission line model shown in Fig. 2(a) can be converted to a lumped-element equivalent circuit model consisting of only capacitors and inductors by substituting lumped-element models for the ENG and MNG layers. A thin ENG layer with an overall thickness of $\Delta\ell$ can be modeled with an inductive T network composed of two series inductors with inductance values of $\frac{1}{2}\mu_0\mu_{\rm ENG}\Delta\ell$ (H) separated by one parallel inductor with an inductance value of $\frac{1}{\epsilon_0(\omega^2_{\rm ENG}-\omega^2)\Delta\ell}$ (H) as shown in Fig. 3(a) [3].

Similarly, a thin MNG layer with a length of $\Delta\ell$ can be represented by a capacitive T network composed of two series capacitors with capacitance values of $\frac{2}{\mu_0(\omega^2_{\rm MNG}-\omega^2)\Delta\ell}$ (F) separated from one another by one parallel capacitor with a capacitance value of $\epsilon_0\epsilon_{\rm MNG}\Delta\ell$ (F) as shown in Fig. 3(b). The equivalent circuit model of a thick MNG layer can be obtained by repeating the T network shown in Fig. 3(b) as shown in Fig. 3(c). This ladder network can be converted to a simple capacitive T network composed of three inductors shown in Fig. 3(c) via consecutive applications of π to T transformation[‖]. Therefore, an MNG layer with arbitrary thickness can be represented by a capacitive network composed of two series capacitors and one parallel capacitor. The capacitor values are obtained by equating the wave transfer matrices of the transmission line model of the thick MNG

[‖] A π to T transformation can convert a circuit composed of one series capacitor sandwiched by two parallel capacitors to a circuit composed of one parallel capacitor sandwiched by two series capacitors.

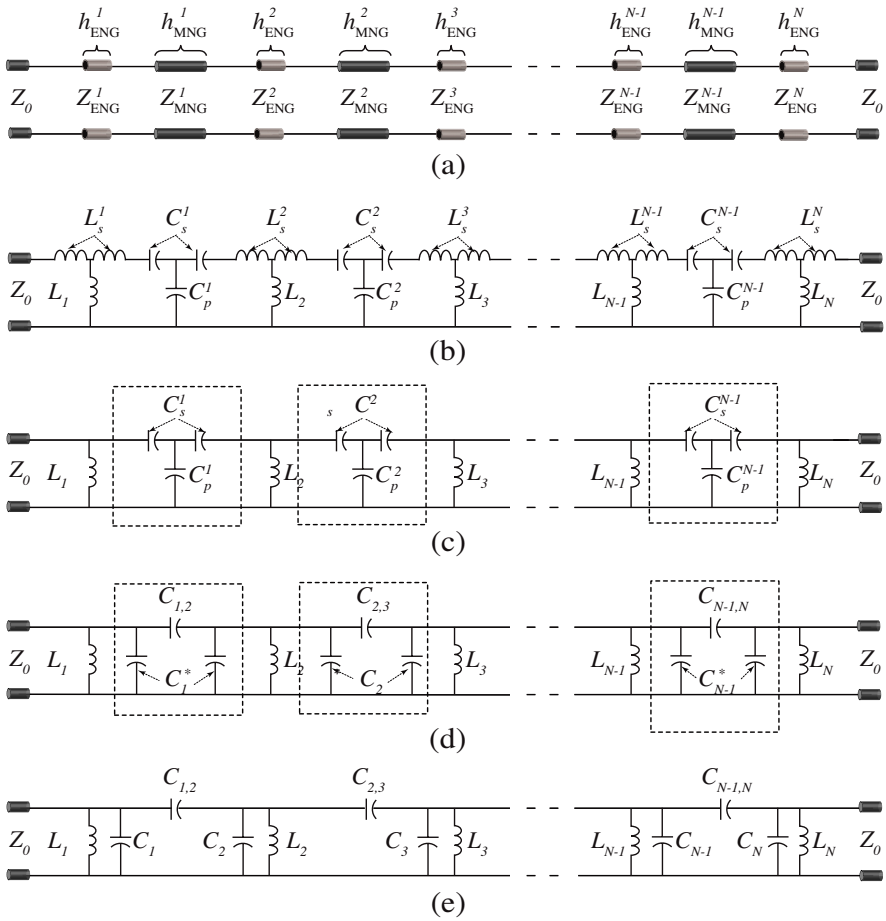

Figure 2. (a) Transmission line model of the multi-layer structure shown in Fig. 1(a) valid for a normally incident TEM wave. (b) The transmission line model of part (a) can be transformed to this equivalent circuit model by substituting lumped-element equivalent circuit models for the ENG and MNG layers. (c) The equivalent LC circuit model of part (b) is simplified to this circuit by ignoring the series inductors L_s^i used in the equivalent circuit model of ENG layers. This is justified when ENG layers are thin. (d) The capacitive T networks highlighted in part (c) can be converted to capacitive π networks highlighted in this figure after a number of T to π transformations. (e) After combining the adjacent parallel inductors of the equivalent circuit network of part (d), the equivalent circuit model of an Nth-order coupled-resonator bandpass filter is obtained.

layer and the capacitive T network shown in Fig. 3(d). These capacitor values are expressed in terms of the parameters of the MNG layer:

$$C_p^i = \frac{\sqrt{\epsilon_{\text{MNG}}^i}\sin\left(\omega\sqrt{\epsilon_0\epsilon_{\text{MNG}}^i\mu_0\mu_{\text{MNG}}^i}h_{\text{MNG}}^i\right)}{\omega Z_0\sqrt{\mu_{\text{MNG}}^i}} \tag{1}$$

$$C_s^i = \frac{C_p^i}{\cos\left(\omega\sqrt{\epsilon_0\epsilon_{\text{MNG}}^i\mu_0\mu_{\text{MNG}}^i}h_{\text{MNG}}^i\right)-1} \tag{2}$$

Note that the values of the above two capacitors depend on frequency. Using the equivalent circuit models for the ENG and MNG layers shown in Figs. 3(a) and 3(d), the transmission-line model shown in Fig. 2(a) can be converted to the lumped-element-based equivalent circuit model shown in Fig. 2(b). Since the ENG layers

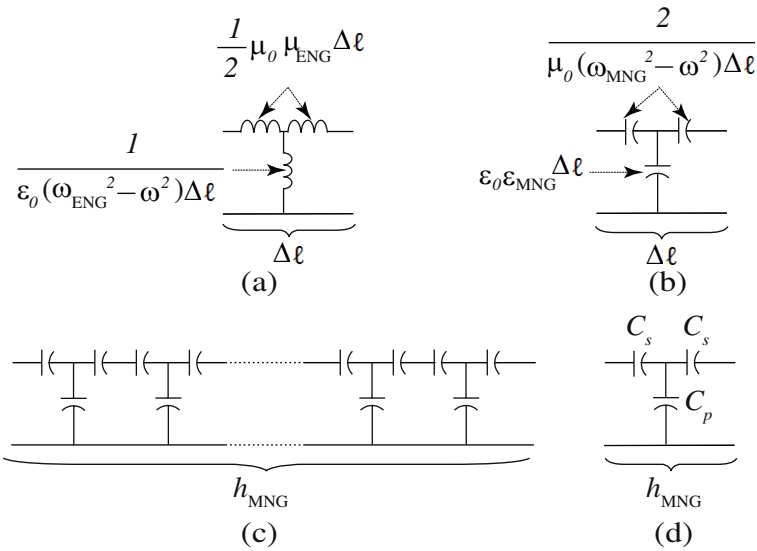

Figure 3. (a) The equivalent circuit model for a short length of an ϵ-negative material with a length of $\Delta\ell \to 0$. (b) The equivalent circuit model for a short length of a μ-negative material with a length of $\Delta\ell \to 0$. (c) The equivalent circuit model of a thick MNG layer can be obtained by cascading the equivalent circuit model shown in part (b) in the form of the ladder capacitive network shown in this figure. (d) Through successive π to T transformations, the capacitive ladder network shown in part (c) can be converted to a single T network. This T network model is valid for an MNG layer with any thickness.

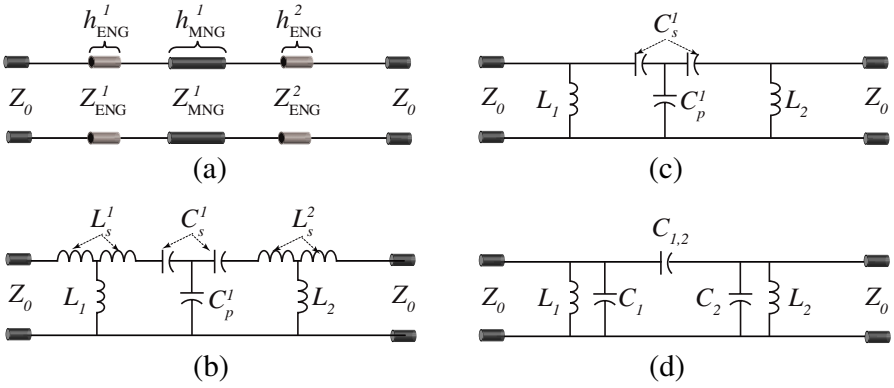

Figure 4. (a) The transmission line model of a tri-layer structure composed of a single MNG layer sandwiched by two ENG layers valid for a vertically-incident TEM wave. (b) The transmission line model of part (a) can be transformed to this circuit by substituting the appropriate lumped-element equivalent circuit models for the MNG and ENG layers as shown in Fig. 3. (c) The network of part (c) is simplified by ignoring the series inductors L_s^1 and L_s^2. This can be done if the thickness of the ENG layers are small. (d) The capacitive T network of part (c) is changed to an equivalent π network to achieve this equivalent circuit model. This circuit is a classical second-order bandpass coupled-resonator filter.

constituting this structure are thin, the values of the series inductors L_s^1, L_s^2, ..., L_s^N are small and they can be ignored to further simplify the structure's equivalent circuit model as shown in Fig. 2(c). Utilizing a T to π transformation, the T networks highlighted in Fig. 2(c) can be converted to the π networks highlighted in Fig. 2(d). After combining the adjacent parallel capacitors (C_i^*) at each node of this circuit, it can be converted to the equivalent circuit model shown in Fig. 2(e), which is a classical, bandpass coupled-resonator filter of order N. Based on the analysis presented above, the structure shown in Fig. 1 is expected to behave as a coupled-resonator bandpass filter if the constituting ENG layers are thin and the frequency of operation is in a range where the ENG and MNG layers have negative permittivity and permeability values respectively. In the subsequent section, we will present an analytical synthesis procedure that relates the desired transmission response of this filter to the physical and geometrical parameters of the multi-layer structure shown in Fig. 1.

3. SYNTHESIS PROCEDURE

3.1. Transmission Through A Single MNG Layer Sandwiched by Two ENG Layers

We will first examine a simple tri-layer structure composed of one MNG layer surrounded by two very thin ENG layers and derive analytical synthesis formulas for this structure. The equivalent circuit model of this tri-layer structure and the analogy between its equivalent circuit model and a second-order, coupled-resonator bandpass filter is illustrated in Figs. 4(a)–(d). Using this analogy a synthesis procedure is developed that allows for obtaining the physical and geometrical parameters of this structure from the characteristics of its desired transmission coefficient. This synthesis procedure is based on determining the parameters of the equivalent circuit model of the structure shown in Fig. 4(d), for a given *a priori* known response, and relating them to the physical and geometrical parameters of the ENG and MNG layers. For the second-order coupled-resonator filter shown in Fig. 4(d), the inductance values L_1 and L_2 are determined from the following equations:

$$L_1 = \frac{\delta Z_0}{\omega_0 q_1} \tag{3}$$

$$L_2 = \frac{\delta Z_0}{\omega_0 q_2} \tag{4}$$

where $\delta = \Delta f / f_0$ is the fractional bandwidth of the transmission window. Δf represents the 3 dB bandwidth of the transmission window (i.e., the difference between frequencies where the magnitude of transmission coefficient decreases from 1 to $\frac{1}{\sqrt{2}}$), and f_0 is the center frequency of operation ($\omega_0 = 2\pi f_0$). After determining the inductance values, the value of the coupling capacitor $C_{1,2}$ can be obtained from:

$$C_{1,2} = \frac{\delta k_{1,2}}{\omega_0^2 \sqrt{L_1 L_2}} \tag{5}$$

where $k_{1,2}$ is the normalized coupling coefficient between the first and second resonators of the coupled-resonator filter shown shown in Fig. 4(d). The values of the normalized quality factors, q_1 and q_2, and the coupling coefficient, $k_{1,2}$, are provided in most filter design handbooks [20]. Finally, the capacitance values of C_1 and C_2 are calculated from:

$$C_{1(2)} = \frac{1}{\omega_0^2 L_{1(2)}} - \frac{\delta k_{1,2}}{\omega_0^2 \sqrt{L_1 L_2}} \tag{6}$$

After determining all lumped element values of coupled-resonator filter shown in Fig. 4(d), the capacitance values of the capacitive T network shown in Fig. 4(c) are obtained after converting the capacitive π to T transformation from:

$$C_s^1 = \frac{C_1C_{1,2} + C_2C_{1,2} + C_1C_2}{C_1} \tag{7}$$

$$C_p^1 = \frac{C_1C_{1,2} + C_2C_{1,2} + C_1C_2}{C_{1,2}} \tag{8}$$

The electric plasma frequencies of the exterior ENG layers are obtained from:

$$f_{\text{ENG}}^{1(2)} = \frac{1}{2\pi}\sqrt{\omega_0^2 + \frac{1}{\epsilon_0 h_{\text{ENG}}^{1(2)} L_{1(2)}}} \tag{9}$$

In this case, the thickness of the ENG layers $h_{\text{ENG}}^{1(2)}$ are assumed to be free design parameters which can be chosen by the designer. The magnetic plasma frequency and the thickness of the MNG layer can be calculated from:

$$f_{\text{MNG}}^1 = \frac{1}{2\pi}\sqrt{\omega_0^2 + \frac{\epsilon_{\text{MNG}}^1\left(2 + \frac{C_p^1}{C_s^1}\right)}{Z_0^2 C_s^1 C_p^1}} \tag{10}$$

$$h_{\text{MNG}}^1 = \frac{\cosh^{-1}\left(1 + \frac{C_p^1}{C_s^1}\right)}{\sqrt{\mu_0\epsilon_0\epsilon_{\text{MNG}}^1\left(\left(2\pi f_{\text{MNG}}^1\right)^2 - \omega_0^2\right)}} \tag{11}$$

Since the equivalent capacitive T network modeling the MNG layer has frequency-dependent capacitors (as demonstrated in (1), (2)), the magnetic plasma frequency and the thickness of the MNG layer predicted by (10) and (11) are frequency dependent as well. To obtain constant values for magnetic plasma frequency and thickness of the MNG layer, ω is replaced by ω_0 in (10) and (11).

3.2. Transmission Through N ENG Layers Separated from One Another by $N-1$ MNG Layers ($N \geq 3$)

The synthesis procedure for the generalized structure shown in Fig. 1 follows a similar procedure as the one described in Section 3.1. First, we will determine the element values of the equivalent circuit model of the structure shown in Fig. 2(e) from the desired filter response of the structure. Then, these element values will be related to those of the circuit model shown in Fig. 2(b) and finally to the geometrical and physical parameters of the MNG and ENG layers of the structure

shown in Fig. 1. With regards to the equivalent circuit model shown in Fig. 2(e), the inductance values of the first and last resonators are determined using:

$$L_{1(N)} = \frac{\delta Z_0}{\omega_0 q_{1(N)}} \tag{12}$$

where q_1 and q_N are the normalized quality factors of the first and last resonators of the filter, respectively. Then, the inductance value of the second resonator is selected to meet the following condition:

$$L_2 > L_1(\delta k_{1,2})^2 \tag{13}$$

The inductance values of inductors L_3, L_4, ..., L_{N-2} must be chosen to satisfy the following condition:

$$L_i > \left(\frac{\delta k_{i-1,i}}{\frac{1}{\sqrt{L_{i-1}}} - \frac{\delta k_{i-2,i-1}}{\sqrt{L_{i-2}}}} \right)^2$$
$$i = 3, 4, \ldots, N-2, \quad i \neq \frac{N+1}{2} \text{ for Odd } N \tag{14}$$

where $k_{i,j}$ represents the normalized coupling coefficient between the ith and jth resonators of the coupled-resonator filter model shown in Fig. 2(e). For odd N values, the inductance value of the middle inductor $L_{\frac{i+1}{2}}$ can be obtained from:

$$\frac{1}{L_{\frac{i+1}{2}}} = \sum_{k=1}^{\frac{i-1}{2}} (-1)^{(k+1)} \frac{1}{L_{\left(\frac{i+1}{2}-k\right)}} + \sum_{k=1}^{\frac{i-1}{2}} (-1)^{(k+1)} \frac{1}{L_{\left(\frac{i+1}{2}+k\right)}}$$
$$i = 3, 5, 7, \ldots, N \quad N\text{: Odd.} \tag{15}$$

For even N values, in addition to the condition specified by (14), the inductance values chosen for L_3, L_4, ..., L_{N-2} must satisfy the following condition:

$$\sum_{k=0}^{\frac{i}{2}-1} (-1)^k \frac{1}{L_{\left(\frac{i}{2}-k\right)}} = \sum_{k=0}^{\frac{i}{2}-1} (-1)^k \frac{1}{L_{\left(\frac{i}{2}+1+k\right)}}$$
$$i = 4, 6, 8, \ldots, N \quad N\text{: Even.} \tag{16}$$

Finally, the value of the inductor of the second to last resonator L_{N-1}, shown in Fig. 2(e), is chosen according to the following condition:

$$L_N \left(\delta k_{N-1,N}\right)^2 < L_{N-1} < \frac{1}{\left(\frac{\delta k_{N-2,N-1}}{\sqrt{L_{N-2}}} + \frac{\delta k_{N-1,N}}{\sqrt{L_N}} \right)^2} \tag{17}$$

The conditions specified in (13)–(17) indicate that the inductor values of the coupled-resonator filter shown in Fig. 2(e) are not unique. In other words, for a given desired frequency response, more than one choice of inductor values exist that results in the desired, *a priori* known, frequency response. This is a consequence of the fact that the coupled-resonator filter shown in Fig. 2(e) is fundamentally an under-determined system. This, however, provides a degree of flexibility in choosing the parameters of the ENG and MNG layers that result in a given response.

After determining all the inductance values of coupled-resonator filter, the capacitance values of the first and last resonators can be obtained from:

$$C_1 = \frac{1}{\omega_0^2 L_1} - \frac{\delta k_{1,2}}{\omega_0^2 \sqrt{L_1 L_2}} \tag{18}$$

$$C_N = \frac{1}{\omega_0^2 L_N} - \frac{\delta k_{N-1,N}}{\omega_0^2 \sqrt{L_{N-1} L_N}} \tag{19}$$

The capacitance values of the remaining resonators are calculated using:

$$C_i = \frac{1}{\omega_0^2 L_i} - \frac{\delta k_{i-1,i}}{\omega_0^2 \sqrt{L_{i-1} L_i}} - \frac{\delta k_{i,i+1}}{\omega_0^2 \sqrt{L_i L_{i+1}}} \quad i = 2, 3, \ldots, N-1. \tag{20}$$

The coupling capacitors can be obtained from:

$$C_{i,i+1} = \frac{\delta k_{i,i+1}}{\omega_0^2 \sqrt{L_i L_{i+1}}} \quad i = 1, 2, \ldots, N-1. \tag{21}$$

The values of the capacitors (C_i^*) shown in Fig. 2(d) can be calculated from:

$$C_1^* = C_1 \tag{22}$$

$$C_{N-1}^* = C_N \tag{23}$$

$$C_i^* = C_i - C_{i-1}^* \quad i = 2, \ldots, N-2. \tag{24}$$

Via a π to T transformation, the series and parallel capacitance values of each T network shown in Fig. 2(c) can be calculated from:

$$C_s^i = \frac{2C_i^* C_{i,i+1} + C_i^* C_i^*}{C_i^*} \tag{25}$$

$$C_p^i = \frac{2C_i^* C_{i,i+1} + C_i^* C_i^*}{C_{i,i+1}} \tag{26}$$

$$i = 1, 2, \ldots, N-1.$$

The electric plasma frequency of the ith ENG layer for a given thickness shown in Fig. 2(a) can be obtained from the previously calculated

inductance values using (27):

$$f^i_{\mathrm{ENG}} = \frac{1}{2\pi}\sqrt{\omega_0^2 + \frac{1}{\epsilon_0 h^i_{\mathrm{ENG}} L_i}} \qquad i = 1, 2, \ldots, N. \tag{27}$$

where h^i_{ENG} is the thickness of the ith ENG layer and its specific value can be chosen arbitrarily[¶]. The thickness and magnetic plasma frequency of ith MNG layer can be related to the capacitance values calculated in the previous steps as shown in the following equations:

$$f^i_{\mathrm{MNG}} = \frac{1}{2\pi}\sqrt{\omega_0^2 + \frac{\epsilon^i_{\mathrm{MNG}}\left(2 + \frac{C^i_p}{C^i_s}\right)}{Z_0^2 C^i_s C^i_p}} \tag{28}$$

$$h^i_{\mathrm{MNG}} = \frac{\cosh^{-1}\left(1 + \frac{C^i_p}{C^i_s}\right)}{\sqrt{\mu_0\epsilon_0\epsilon^i_{\mathrm{MNG}}\left(\left(2\pi f^i_{\mathrm{MNG}}\right)^2 - \omega_0^2\right)}} \tag{29}$$

$$i = 1, 2, \ldots, N-1.$$

(28) and (29) show that the magnetic plasma frequency and the thicknesses of the MNG layers are frequency dependent. Similar to the process followed in Section 3.1, ω is replaced by ω_0 in(28) and (29) to obtain constant values of the thickness and the magnetic plasma frequency.

4. VERIFICATION OF THE SYNTHESIS PROCEDURE USING FULL-WAVE EM SIMULATIONS

4.1. Transmission through a Single MNG Layer Sandwiched by Two ENG Layers

In our first design example, we consider a three-layer structure composed of one MNG layer sandwiched by two ENG layers on the two sides. Using the synthesis procedure presented in Section 3.1, we will determine the geometrical and physical parameters of different MNG and ENG layers that result in a flat transmission coefficient (a Butterworth filter response) with a center frequency of operation of 2.4 GHz and a fractional bandwidth of $\delta = 20\%$. Table 1 shows the normalized quality factors and the normalized coupling coefficient of an ideal coupled-resonator filter with a second-order Butterworth response. In this synthesis procedure, the relative permeability of the

[¶] The chosen value of h^i_{ENG} must be as small as possible to ensure that the approximations described in Section 2 remain valid.

Table 1. Normalized quality factors and coupling coefficients of the coupled-resonator bandpass filters examined in this paper.

Filter Type	Order (N)	δ	q_1	q_N	r_1
Butterworth	2	20%	1.4142	1.4142	1
Chebychev (0.5 dB ripple)	5	40%	1.8068	1.8068	1
Filter Type	r_N	$k_{1,2}$	$k_{2,3}$	$k_{3,4}$	$k_{4,5}$
Butterworth	1	0.7071			
Chebychev (0.5 dB ripple)	1	0.6519	0.5341	0.5341	0.6519

ENG layer, μ_{ENG}, and the relative permittivity of the MNG layer, ϵ_{MNG}, can be chosen arbitrarily. Close examination of the procedures presented in Sections 3.1 and 3.2 reveals that choosing small μ_{ENG} values enhances the agreement between the response of the proposed structure and an ideal coupled-resonator filter response. This is due to the fact that the values of the series inductors L_S^i shown in Fig. 2(b) and Fig. 4(b) are directly proportional to μ_{ENG}^i. Since the effect of these series inductors are ignored in the proposed synthesis procedure, choosing small relative permeability values reduces the impact of this assumption. Therefore, in this synthesis procedure, we choose $\mu_{\text{ENG}} = 1$.

Similarly, by examining the synthesis procedures presented in Sections 3.1 and 3.2, the effect of choosing specific ϵ_{MNG} values on the accuracy of the proposed synthesis procedure can be evaluated. In particular, (10) and (28) show that ϵ_{ENG} can significantly influence the value of the magnetic plasma frequency. Since the proposed synthesis procedure is based on the assumption that the entire operating frequency band of interest falls below the magnetic plasma frequency of the MNG material, the choice of ϵ_{MNG} can influence the validity of this procedure. Thus, (10) suggests that ϵ_{MNG} should be chosen as large as possible to enhance the accuracy of the proposed synthesis procedure. For the three-layer structure described above, if the synthesis procedure is carried out with $\epsilon_{\text{MNG}} = 1$, (10) predicts f_{MNG} to be 2.42 GHz (the values of the remaining physical and geometrical parameters of this structure are shown in Table 2). This value of f_{MNG} is in the middle of the desired transmission window. Above f_{MNG}, the transmission-line model shown in Fig. 2(a) will no longer be equivalent to that shown in Fig. 2(b) and the entire synthesis procedure falls apart. The effect of ϵ_{MNG} on the proposed synthesis procedure is

Table 2. Physical parameters and dimensions of the tri-layer structures studied in Section 3.1.

	$h_{\mathrm{ENG}}^{1,2}$	$f_{\mathrm{ENG}}^{1} = f_{\mathrm{ENG}}^{2}$	h_{MNG}	f_{MNG}	ϵ_{MNG}
Case 1	500 μm	40.3 GHz	368 mm	2.42 GHz	1
Case 2	500 μm	40.3 GHz	36.8 mm	2.63 GHz	10
Case 3	500 μm	40.3 GHz	3.68 mm	4.19 GHz	100
Case 4	500 μm	40.3 GHz	1.84 mm	5.41 GHz	200
Case 5	100 μm	90.0 GHz	1.84 mm	5.41 GHz	200
Case 6	10 μm	284.5 GHz	1.84 mm	5.41 GHz	200

examined by designing the aforementioned tri-layer structure for four different ϵ_{MNG} values. Following the synthesis procedure presented in Section 3.1, the parameters of this structure are obtained for $\epsilon_{\mathrm{MNG}} = 1$, 10, 100, and 200 and the results are presented in Table 2 (Case 1–Case 4). The frequency response of these structures are calculated using full-wave numerical EM simulations in CST studio and the results are presented in Fig. 5. As can be seen, by increasing ϵ_{MNG}, the agreement between the response of the ideal filter and that of the tri-layer structure is improved as expected.

The thickness of the (thin) ENG layers constituting the structure, h_{ENG}, is another design parameter that can be chosen freely. To examine the effect of this design parameter on the frequency response of the tri-layer structure examined here, three different structures with different h_{ENG} values are designed following the synthesis procedure presented in Section 3.1. The physical parameters of these are provided in Table 2 (Case 4–Case 6) and their frequency responses are calculated in CST Microwave Studio. Figure 6 shows the simulated frequency responses of these structures as well as the frequency response of the ideal coupled-resonator bandpass filter with a second-order Butterworth response with $f_0 = 2.4\,\mathrm{GHz}$ and $\delta = 20\%$. As can be seen, in general, a good agreement is observed between the ideal filter responses and the transmission coefficients of the ENG-MNG structures. Additionally, it can be observed that as h_{ENG} decreases, the agreement between the simulated transmission coefficients and the ideal filter response improves as described earlier in this sub-section. Based on the results shown in Figs. 5 and 6, it can be seen that the equivalency between the multi-layer structure shown in Fig. 1 and an Nth-order coupled-resonator bandpass filter is best when the ENG layers are extremely thin and the MNG layers have high relative permittivity values.

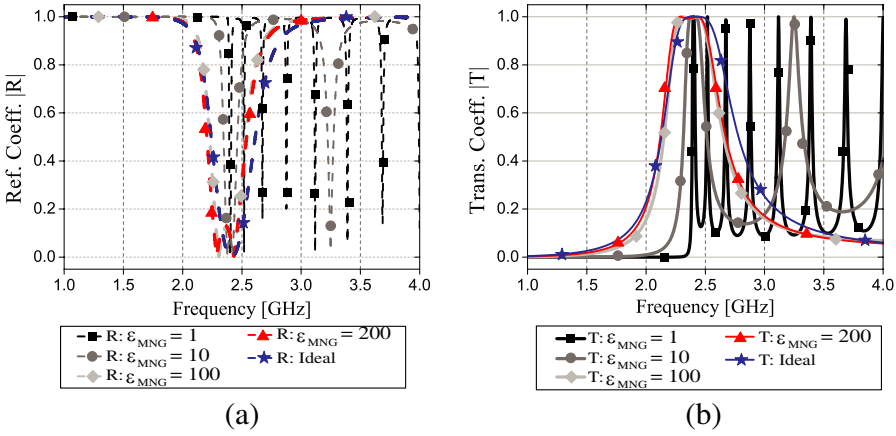

Figure 5. The (a) reflection and (b) transmission coefficients of the tri-layer structure studied in Section 4.1 for different ϵ_{MNG} values obtained using full-wave EM simulations in CST Microwave Studio. The desired (ideal) filter response is also shown as reference. The physical parameters of the structures are provided in Table 2 (Case 1–Case 4). These results show the effect of the dielectric constant of the MNG layer of a tri-layer structure (ENG-MNG-ENG) on the accuracy of the synthesis procedure described in Section 3.1.

4.2. EM Wave Tunneling through Four MNG Layers Sandwiched by Five ENG Slabs

The second structure that we consider in this paper is a multi-layer structure composed of four MNG layers sandwiched by five ENG layers. Following the synthesis procedure of Section 3.2, we seek to determine the physical and geometrical parameters of the structure that results in an equal-ripple transfer function centered at 2.4 GHz with a fractional bandwidth of $\delta = 40\%$. As described in Section 3.2, the multi-layer structure shown in Fig. 1 with N ENG layers is equivalent to an Nth-order banspass filter. Therefore, in synthesizing the proposed structure, the parameters of a fifth-order coupled-resonator bandpass filter with an equal-ripple response type, shown in Table 1, are used. As described in Section 2, such a fifth-order bandpass filter is an under-determined system and more than one combination of element values exist that result in a given transfer function. Table 3 shows the element values of the equivalent circuit model of this filter determined from (12)–(21). Using these values in conjunction with (22)–(29), the physical parameters of the different ENG and MNG layers constituting the structure are calculated and the results are presented in Table 4.

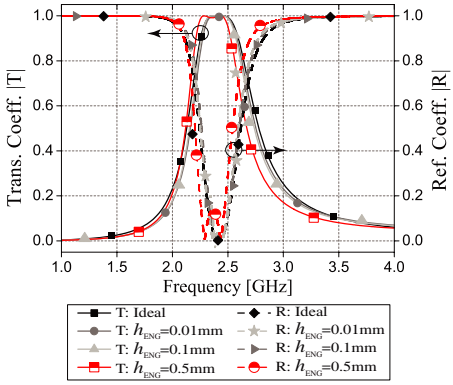

Figure 6. The transmission and reflection coefficients of the tri-layer structure composed of one MNG layer sandwiched by two ENG layers discussed in Section 4.1 obtained using full-wave EM simulations in CST Studio. The desired (ideal) filter response is also shown for comparison. The physical parameters of the structures are given in Table 2 (Case 4–Case 6).

The transmission and reflection coefficients of this multi-layer structure are also calculated using full-wave numerical EM simulations in CST Microwave studio and presented in Fig. 7. Additionally, Fig. 7 shows the transmission and reflection coefficients of an ideal coupled-resonator filter with a fifth-order equal-ripple response. As can be observed, in general, a good agreement between the two results is observed. The discrepancies can be attributed to the finite thickness of the ENG layers as well as the effect of ϵ_{MNG} on the accuracy of the response as described in Section 3.1. Close examination of the ideal filter response shown in Fig. 7 shows that the ripples in the transmission coefficient of the filter are not of equal magnitude. This is due to the fact that the well-known coupled-resonator filter synthesis procedure that we used in this work is based on a narrow-band approximation [20]. As the bandwidth of the filter increases, the accuracy of this approximation reduces as can be observed from the transfer function of the ideal filter shown in Fig. 7. Nonetheless, the transmission coefficient of the multi-layer ENG-MNG structure closely follows the response of the ideal filter as expected.

4.3. The Effect of Loss

Complete transmission of EM waves through the multi-layer structure shown in Fig. 1 is only possible when the structure is lossless. In

Table 3. Equivalent circuit values of the fifth-order coupled-resonator filter of the type shown in Fig. 2(e), which is studied in Section 3.2.

Parameter	$C_1 = C_5$	$C_2 = C_4$	C_3	$L_1 = L_5$
Value	0.502 pF	0.957 pF	0.91 pF	5.535 nH
Parameter	$L_2 = L_4$	L_3	$C_{1,2} = C_{4,5}$	$C_{2,3} = C_{3,4}$
Value	2.767 nH	2.767 nH	0.29 pF	0.34 pF

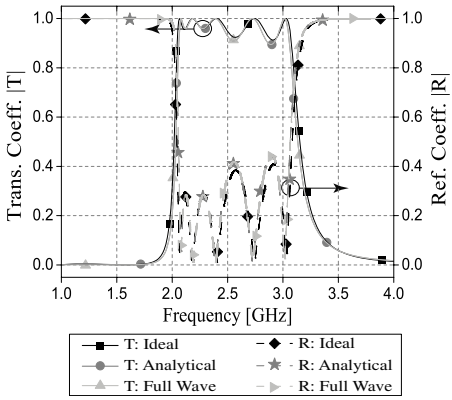

Figure 7. The transmission and reflection coefficients of the multi layer structure composed of four MNG layers sandwiched by five ENG layers discussed in Section 4.2 obtained from full-wave EM simulations in CST Studio. The desired (ideal) filter response is also shown for comparison. The physical parameters of this structures are given in Table 4.

reality, however, both the ENG and MNG layers will be lossy. In the Drude model used for ϵ_{ENG} (μ_{MNG}), this loss can be modeled by considering the relative permittivity (relative permeability) of the ENG (MNG) material to be a complex number. This can be done by considering a nonzero electric (magnetic) collision frequency term, ν_{ENG} (ν_{MNG}), in the Drude model used for the relative permittivity (relative permeability) of the ENG (MNG) materials:

To demonstrate the effect of the material loss on the response of the structure, the total power loss of several multi-layer structures of the type shown in Fig. 1 are calculated and the results are presented in Fig. 8. In obtaining these results, it is assumed that all of these structures have a Butterworth response type centered at 2.4 GHz and use lossy ENG and MNG layers with $\nu_{\text{ENG}}/\omega = 0.005$ and $\nu_{\text{MNG}}/\omega = 0.005$. Figure 8 shows the percentage of the incident power

Table 4. Physical parameters of the nine-layer ENG-MNG composite structure examined in Section 3.2.

Parameter	$f^1_{\mathrm{ENG}} = f^5_{\mathrm{ENG}}$	$f^2_{\mathrm{ENG}} = f^3_{\mathrm{ENG}} = f^4_{\mathrm{ENG}}$	h_{ENG}	ϵ_{MNG}
Value	227.3 GHz	321.6 GHz	10 μm	200
Parameter	$h^1_{\mathrm{MNG}} = h^4_{\mathrm{MNG}}$	$f^1_{\mathrm{MNG}} = f^4_{\mathrm{MNG}}$	$h^2_{\mathrm{MNG}} = h^3_{\mathrm{MNG}}$	$f^2_{\mathrm{MNG}} = f^3_{\mathrm{MNG}}$
Value	690.7 μm	8.4 GHz	606.6 μm	8.7 GHz

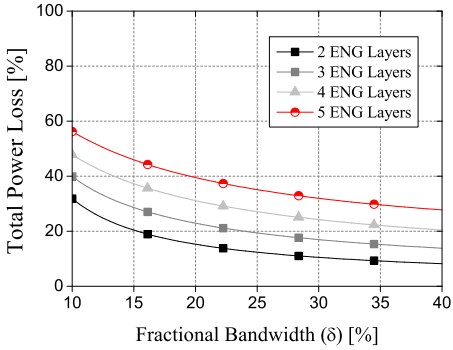

Figure 8. The percentage of the total power lost in the multi-layer structure shown in Fig. 1 as a function of the number of ENG layers, N, and the fractional bandwidth, δ. The results are obtained for multi-layer structures exhibiting a maximally flat bandpass response centered at 2.4 GHz. It is assumed that the ENG and MNG materials are lossy with $\nu_{\mathrm{ENG}}/\omega = \nu_{\mathrm{MNG}}/\omega = 0.005$.

lost in the structure as a function of the fractional bandwidth of the transmission window as well as the number of ENG layers, $N^\sharp$. As can be observed, the power loss increases with increasing the number of the layers (i.e., the order of the filter) and reduces with increasing the fractional bandwidth of the transmission window. This trend is consistent with the behavior of microwave filters, where losses increase with decreasing the bandwidth of the filter and increasing the order of the filter response [21].

$^\sharp$ The number of MNG layers is $N - 1$.

5. EM WAVE TUNNELING THROUGH THE DUAL MULTI-LAYER MNG-ENG STRUCTURE

If we apply the duality principle to the structure shown in Fig. 1, a new multi-layer structure can be obtained in which N MNG layers sandwich $N-1$ ENG layers. This transforms the problem shown in Fig. 1 to that shown in Fig. 9. This change, however, does not change the response of the structure. Following a similar analysis procedure as the one presented in Section 2, it can be shown that the dual structure shown in Fig. 9 is analogous to a coupled-resonator filter composed of series LC resonators coupled to each other using parallel inductors as depicted

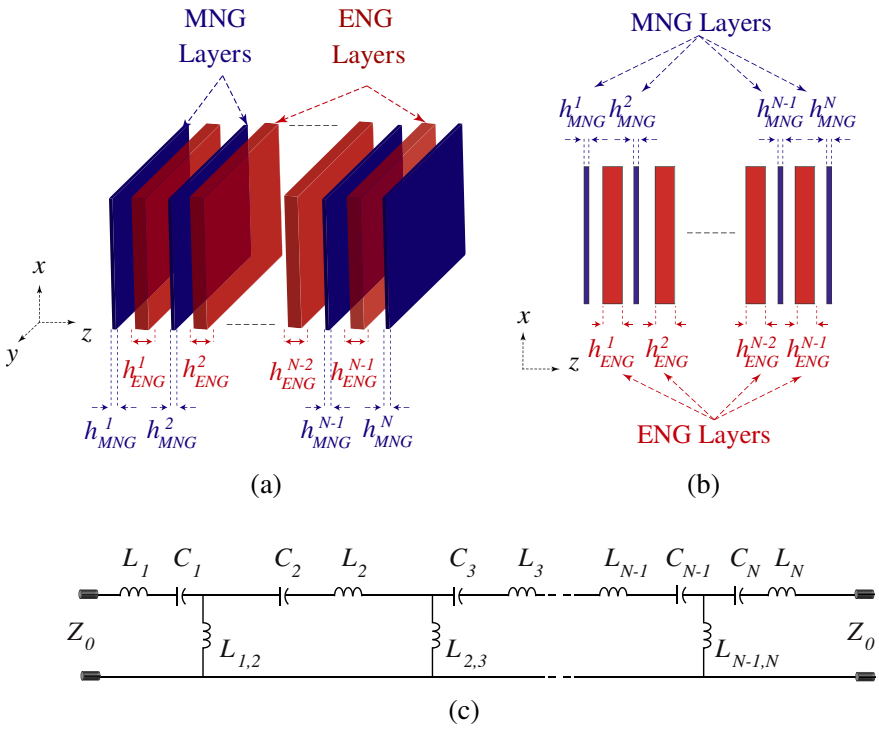

Figure 9. (a) 3D topology of the multi-layer structure that is dual of the one shown in Fig. 1. In this case, the structure is composed of N MNG layers separated from each other by $N-1$ ENG layers. (b) Side view of the dual structure. (c) Following a procedure similar to that described in Section 2, it can be shown that the multi-layer structure of parts (a)–(b) can be modeled with a coupled-resonator filter composed of series LC resonators coupled to each other using parallel inductors.

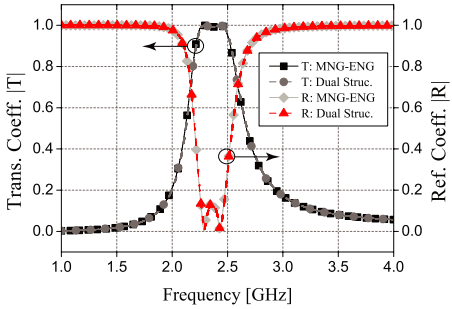

Figure 10. The transmission and reflection coefficients of the tri-layer structure discussed in Section 4.1 and its dual structure examined in Section 5. These results are obtained from full-wave EM simulation in CST Studio and show perfect agreement. The physical parameters of the structures are presented in Table 2 (Case 4).

in Fig. 9(c). This coupled-resonator filter is in fact dual of the circuit shown in Fig. 2(e). Rather than developing a new synthesis procedure for this structure, the synthesis procedure presented in Section 3 can be used in conjunction with the duality principle to synthesize structures of the type shown in Fig. 9. This can be demonstrated by examining the dual of the tri-layer structure described in Section 4.1. The dual structure is composed of an ENG layer sandwiched by two MNG layers. The parameters of this multi-layer structure are provided in Table 2 (Case 4 after exchanging the ENG subscripts MNG and vice versa). The response of this structure is also calculated using full-wave EM simulations in CST Microwave Studio. Figure 10 shows the reflection and transmission coefficients of this structure and compares them with those of the tri-layer structure examined in Section 3.1 (with two ENG and one MNG layers). As expected, the results match perfectly.

6. CONCLUSIONS

In this paper, we examined the close relationship that exists between EM wave tunneling through stacks of single-negative metamaterial slabs and two classical coupled-resonator microwave filters. We demonstrated that a structure composed of N thin ENG layers separated from each other by $N-1$ MNG layers is equivalent to a capacitively-coupled, coupled-resonator filter with an Nth-order bandpass response. Assuming Drude dispersion models for the relative permittivity (permeability) of the ENG (MNG) layers, we developed an analytical synthesis procedure and showed that it can be used

to determine the physical parameters of these multi-layer structures from their *a priori* known desired transfer functions. Using this synthesis procedure, we found out that the MNG layers must have high relative dielectric constant values to ensure that their magnetic plasma frequencies will not fall within the desired transmission window (and hence, invalidate the assumption that the materials have negative permeability values). This condition is a consequence of the specific dispersion model assumed for the MNG material. Several design examples were used in conjunction with full-wave EM simulations to demonstrate the validity of the proposed analogy and examine the accuracy of the proposed synthesis procedure. The conclusions of the main study were also expanded to the dual problem using the duality principle.

REFERENCES

1. Tai, G. C., Y. W. Kiang, and C. H. Chen, "Plasma-dielectric sandwich structure used as a tunable bamlpass microwave filter," *IEEE Trans. on Microw. Theory and Techn.*, Vol. 32, 111–113, 1984.
2. Dragila, B., B. Luther-Davies, and S. Vukovic, "High transparency of classically opaque metallic films," *Phys. Rev. Lett.*, Vol. 55, 1117–1120, 1985.
3. Alu, A. and N. Engtheta, "Pairing an epsilon-negative slab with a mu-negative slab: resonance, tunneling and transparency," *IEEE Trans. on Antennas and Propag.*, Vol. 51, 2558–2571, 2003.
4. Alu, A. and N. Engtheta, "Guided modes in a waveguide filled with a pair of single-negative (SNG), double-negative (DNG), and/or double-positive (DPS) layers," *IEEE Trans. on Microw. Theory and Techn.*, Vol. 52, 199–210, 2004.
5. Jiang, H., H. Chen, H. Li, Y. Zhang, J. Zi, and S. Zhu, "Properties of one-dimensional photonic crystals containing single-negative materials," *IEEE Trans. on Phys. Rev. E*, Vol. 69, 066607, 2004.
6. Kim, K. Y., "Photon tunneling in composite layers of negative- and positive-index media," *Phys. Rev. E*, Vol. 70, 047603, 2004.
7. Kim, K. Y., "Properties of photon tunneling through single-negative materials," *Opt. Lett.*, Vol. 30, 430–432, 2005.
8. Alu, A. and N. Engtheta, "Evanescent growth and tunneling through stacks of frequency-selective surfaces," *IEEE Antennas and Wireless Propag. Lett.*, Vol. 4, 417–420, 2005.
9. Zhou, L., W. Wen, C. T. Chen, and P. Sheng, "Electromagnetic

wave tunneling through negative-permittivity media with high magnetic fields," *Phys. Rev. Lett.*, Vol. 94, 243905, 2005.

10. Hooper, I. R., T. W. Preist, and J. R. Sambles, "Making tunnel barriers (including metals) transparent," *Phys. Rev. Lett.*, Vol. 97, 053902, 2006.
11. Alu, A., N. Engtheta, and R. W. Ziolkowski, "Transmission-line analysis of epsilon-near-zero (ENZ)-filled narrow channels," *Phys. Rev. E*, Vol. 74, 016604, 2006.
12. Guan, G., H. Jiang, H. Li, H. Zhang, H. Chen, and S. Zhu, "Tunneling modes of photonic heterostructures consisting of single-negative materials," *Appl. Phys. Lett.*, Vol. 88, 211112, 2006.
13. Kim, K. Y. and B. Lee, "Complete tunneling of light through impedance-mismatched barrier layers," *Phys. Rev. A*, Vol. 77, 023822, 2008.
14. Feng, T., Y. Li, H. Jiang, Y. Sun, H. Li, Y. Zhang, Y. Shi, and H. Chen, "Electromagnetic tunneling in a sandwich structure containing single negative media," *Phys. Rev. E*, Vol. 79, 026601, 2009.
15. Ding, Y., Y. Li, H. Jiang, and H. Chen, "Electromagnetic tunneling in nonconjugated epsilon-negative and mu-negative metamaterial pair," *PIERS Online*, Vol. 6, 109–112, 2010.
16. Butler, C. A. M., I. R. Hooper, A. P. Hibbins, J. R. Sambles, and P. A. Hobson, "Metamaterial tunnel barrier gives broadband microwave transmission," *J. Appl. Phys.*, Vol. 109, 013104, 2011.
17. Al-Joumayly, M. and N. Behdad, "A generalized method for synthesizing low-profile, band-pass frequency selective surfaces with non-resonant constituting elements," *IEEE Trans. on Antennas and Propag.*, Vol. 58, 4033–4041, 2010.
18. Castaldi, G., I. Gallina, V. Galdi, A. Alu, and N. Engheta, "Electromagnetic tunneling through a single-negative slab paired with a double-positive bilayer," *Phys. Rev. B*, Vol. 83, 081105, 2011.
19. Castaldi, G., I. Gallina, V. Galdi, A. Alu, and N. Engheta, "Transformation-optics generalization of tunneling effects in bilayers made of paired epsilon-negative/mu-negative media," *J. Opt.*, Vol. 13, 024011, 2011.
20. Zverev, A. I., *Hankbook of Filter Synthesis*, Wiley-Interscience, New York, 1967.
21. Cameron, R. J., *Microwave Magazine*, Vol. 12, 42, 2011.